

ARTICLE OPEN



Drought characteristics in Mediterranean under future climate change

Yassmin H. Essa^{1,2}✉, Martin Hirschi³, Wim Thiery⁴, Ahmed M. El-Kenawy⁵ and Chunxue Yang¹

The present work aims to address the physical properties of different drought types under near-future climates in the Mediterranean. To do so, we use a multi-model mean of the bias-adjusted and downscaled product of five Earth System Models participating in the Coupled Model Intercomparison Project—phase6 (CMIP6), provided by Inter-Sectoral Impact Model Intercomparison Project (ISIMIP), under four shared socioeconomic pathways (SSP1–2.6, SSP2–4.5, SSP3–7.0, and SSP5–8.5) for the period 2021–2060, to estimate the Standardized Precipitation Evapotranspiration Index (SPEI) at 1-, 6-, and 12-month time scales, and address the meteorological, agricultural, and hydrological drought, respectively. Additionally, SPEI is calculated from the bias-adjusted CMIP6 historical simulations and the reanalysis ‘WFDE5’ for 1980–2014 as a historical and reference period. The comparison of the CMIP6 with WFDE5 reveals a consistently increasing tendency for drought occurrences in the Mediterranean, particularly for agricultural and hydrological drought time scales. Nonetheless, an overestimation in historical trend magnitude is shown by the CMIP6 with respect to WFDE5. The projection results depict drought frequencies ranging between 12 and 25% of the studied period 2021–2060, varying with regions and climate scenarios. The tendency to increase the drought frequency is more pronounced in the southern than northern Mediterranean countries. Drought severity is remarkable in the aggregated time scales; consequently, more pressure is foreseen in the food and water sectors. Drought seasonality reveals a higher tendency for drought occurrences in summer (autumn) months for the meteorological (agricultural) droughts. The driving factor(s) for drought occurrence strongly depends on regional climate characteristics.

npj Climate and Atmospheric Science (2023)6:133; <https://doi.org/10.1038/s41612-023-00458-4>

INTRODUCTION

Drought is a complex climate-related phenomenon that can significantly impact the agricultural and hydrological sectors and increase environmental and socioeconomic risk. It is characterized based on duration, frequency, and intensity^{1,2}. For example, the persistence of short-term dry meteorological conditions, i.e., within a few weeks, is classified as a ‘meteorological drought.’ Extending the dry conditions for a longer period, 3–9 months, can affect the soil moisture and vegetation and is classified as an ‘agricultural drought’³. Longer than 9 months of dryness, the impact will transfer to the hydrological systems, which is classified as a ‘hydrological drought’⁴. Increasing the frequency of drought events, particularly for agricultural and hydrological types, can alter the socioeconomic and the ecosystem⁵.

As reported in the Sixth Assessment Report of the Intergovernmental Panel on Climate Change⁶, a significant change (medium to high confidence) toward increasing agricultural and hydrological drought frequency is observed in the Mediterranean. The Mediterranean has also been marked as a hotspot region for climate change in several recent studies [e.g.,^{7,8}]. Evidence from the available records and recent studies show increasing drought frequencies in the last decades in Mediterranean countries [e.g.,⁹]. Recently, Northern Mediterranean experienced a dramatic drought in 2022 correlated to the consequences of extreme heatwaves and a long-lasting deficit in precipitation, causing a significant reduction in major crop production and river discharge, as reported by Global Drought Observatory¹⁰. Beyond the historical and current conditions, the projected warming rate in the Mediterranean during the summertime is expected to be 50%

larger than global annual warming and 20% larger at the annual time scale⁶.

The Mediterranean climate is classified as ‘*csa*’ according to the Koppen climate classification, which is characterized by hot-dry summer and mild-wet winter as a result of the interactions between mid-latitude and tropical processes¹¹. This contrast between the North African (arid climate) and European continental (temperate-rainy) climates within the Mediterranean domain adds more complexity to understanding the impacts of climate change in this region^{12,13}. Additionally, the large variability related to the socioeconomic conditions in the Mediterranean countries can increase the challenges for developing effective adaptation strategies^{14,15}.

Concurrently, drought quantification is still challenging since it cannot be directly measured based on one variable^{16,17}, but it is usually identified by its effects or by its impacts on different types of systems. Therefore, drought is often quantified indirectly using indices. Those indices’ efficiency is based on each region’s climate characteristics. For example, indices that depend only on precipitation have shown limitations in detecting drought in arid and semi-arid areas^{18,19}. Another limitation of the precipitation single-dependence indices is that they neglect the role of temperature in increasing water loss through enhanced evaporation^{20–22} and the impact of global warming on drought characteristics^{23,24}. Instead, indices that combine precipitation and temperature or atmospheric evaporative demand (AED) have been proposed and have proven effective in drought detection^{17,25–28}.

¹Institute of Marine Sciences (ISMAR), National Research Council (CNR), Rome, Italy. ²Central Laboratory for Agricultural Climate (CLAC), Agricultural Research Center (ARC), Giza, Egypt. ³Institute for Atmospheric and Climate Science, ETH Zurich, Zurich, Switzerland. ⁴Department of Hydrology and Hydraulic Engineering, Vrije Universiteit Brussel (VUB), Brussels, Belgium. ⁵Instituto Pirenaico de Ecología, Consejo Superior de Investigaciones Científicas (IPE-CSIC), Zaragoza, Spain. ✉email: Yassmin.hesham@artov.ismar.cnr.it

SPEI drought frequency decadal trend 1980–2014

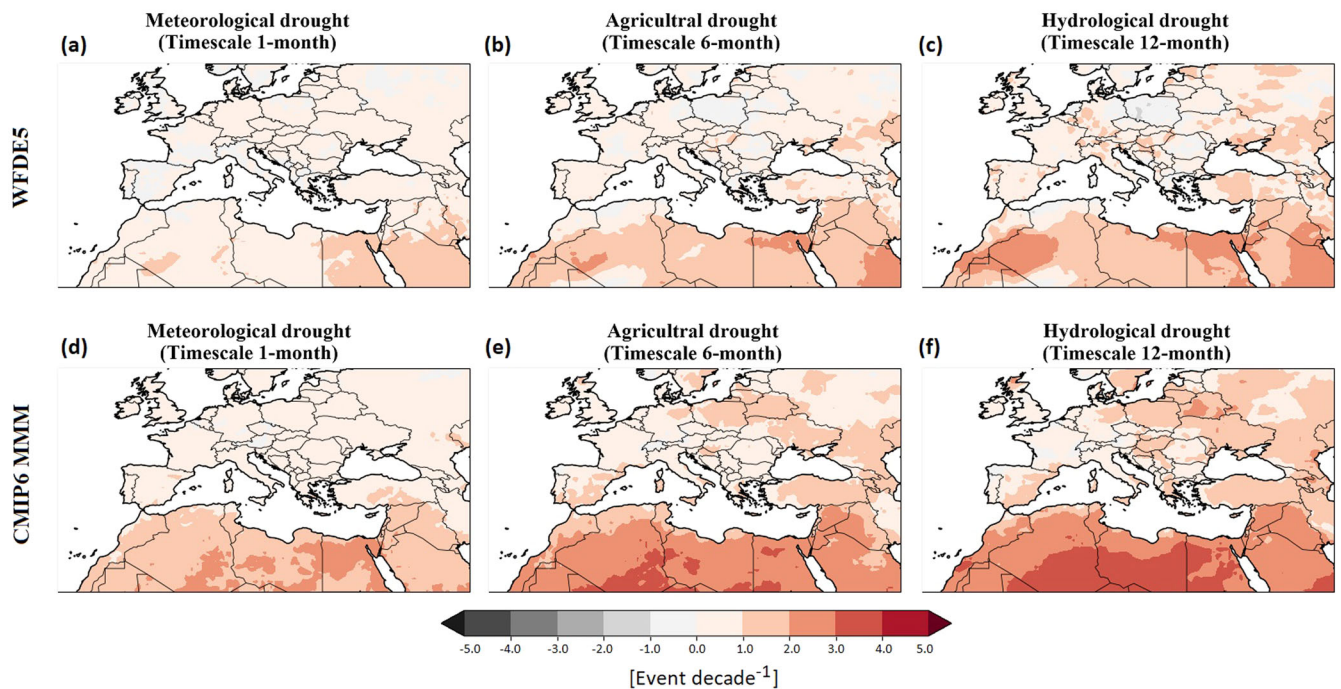


Fig. 1 Historical drought trends. Drought frequency trend during the baseline period 1980–2014, based on SPEI value at time scales **a, d** 1-month, **b, e** 6-months, and **c, f** 12-months from WFDE5 (top) and CMIP6 MMM (bottom).

Previous studies have discussed the projected drought in detail on regional scales [e.g. ^{15,29–31}], yet these studies were either using mainly precipitation-based indices, neglecting the impact of temperature on their assessment, or based on the older generations of the Coupled Model Intercomparison Project, i.e., phase 3 (CMIP3) or phase 5 (CMIP5). The major outcomes from these studies highlighted the potential increase in drought frequency and severity in the future; however, large uncertainties in drought projection by CMIP3 and CMIP5 have been reported in the fifth assessment report of the IPCC^{32,33}. Additionally, substantial disagreements in meteorological drought trends by the CMIP5 ensemble compared with observations are reported^{34,35}, including a tendency to overestimate drying, particularly in mid-to-high latitudes³⁴. Currently, the updated models' outputs of phase 6 (CMIP6³⁶) have become available, and the indices of detecting drought have matured, allowing a more robust assessment of the drought projection.

Significant change is reported in the CMIP6 compared to CMIP5, particularly regarding precipitation patterns³⁷ on both global and regional scales³⁸, which can have important implications for future drought projections. Recent studies have reported improvement in CMIP6's ability compared to CMIP5 in representing climate features such as extreme heat, precipitation, El Niño Southern Oscillation (ENSO), and the monsoon^{39–43}. CMIP6 also uses the new shared socioeconomic pathways (SSPs)⁴⁴ to simulate climate change scenarios. SSPs describe different socioeconomic reference assumptions and are combined with representative concentration pathways (RCPs) to provide a better representation of the future scenario^{45,46}.

Recent studies^{47–49} used CMIP6 to assess drought under climate change from a global perspective, large-scale wet and dry pattern, addressing the similarities and discrepancies with older CMIP generations. To the best of our knowledge, the studies conducted to address the future drought projection over the Mediterranean regional scale using CMIP6 and the new future scenarios are limited, and they rely on the low spatial resolution of the global

models. The main objective of this study is to investigate the physical properties of different drought types (i.e., meteorological, agricultural, and hydrological) in the Mediterranean and provide a detailed description of the potential profile for the near future. To this aim, we use multi-model mean (MMM) of five bias-adjusted and downscaled to a high-resolution output ($0.5^\circ \times 0.5^\circ$) of CMIP6 Earth System Models (ESMs) compared to the original output resolution (Supplementary Table 2) and widely-used index, Standardized Precipitation-Evapotranspiration Index SPEI⁵⁰, to address drought characteristics over the Mediterranean. SPEI combines precipitation and AED to examine the impact of climate on the water balance. Furthermore, it is a multi-scalar index that allows the investigation of different drought types and multi-dimensional analysis (i.e., duration, timing, and intensity dimensions) that is widely used for studying temperature and rainfall extremes^{51–53}. For these reasons, SPEI is preferred over other indices, as well as supported by the IPCC Sixth Assessment Report.

RESULTS

Drought frequency and severity

Figure 1 shows the linear trend of the drought frequency during the historic period, 1980–2014, based on SPEI at time scales of 1, 6, and 12 months for the meteorological, agricultural, and hydrological droughts, respectively, using the bias-corrected reanalysis WFDE5 and the CMIP6 MMM (detailed description in “Methods” section). The obtained results reveal a consistently increasing tendency for dry events in the Mediterranean over the past 35 years in both datasets, particularly the agricultural and hydrological drought time scales (i.e., 6 and 12 months). Moreover, in both datasets, this tendency is more pronounced in the southern Mediterranean (North African countries) than in the Northern ones (southern EU). This result depicts the homogeneity of the employed CMIP6 MMM with respect to WFDE5 and demonstrates

Drought frequency for the period 2021 - 2060

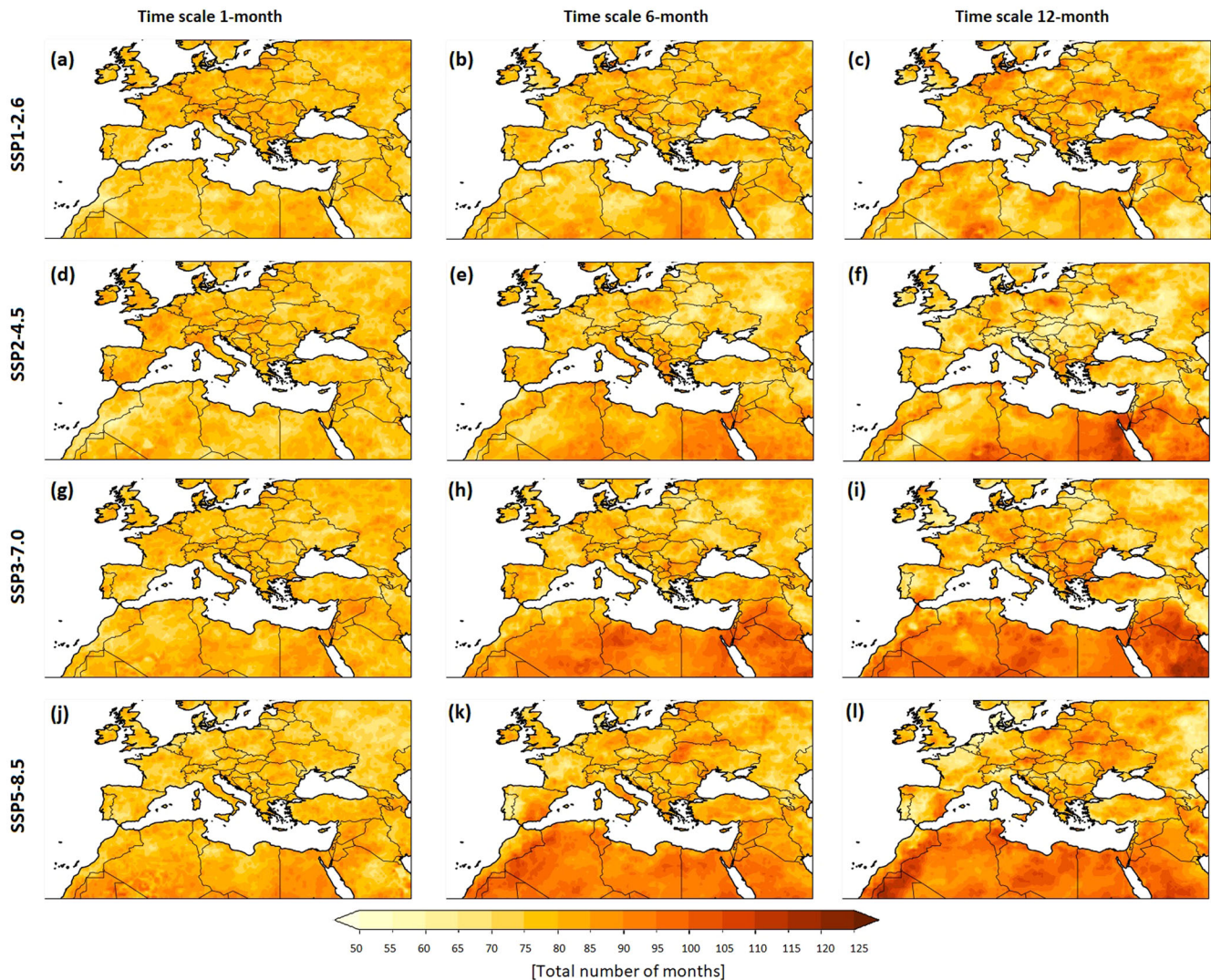


Fig. 2 Projected drought frequency. Drought frequency based on the SPEI at time scales of 1, 6, and 12 months, spanning the projection period 2021–2060 from the CMIP6 MMM under the climate change scenarios SSP1–2.6 (a–c), SSP2–4.5 (d–f), SSP3–7.0 (g–i), and SSP5–8.5 (j–l).

its reliable performance to be used for investigating the projected drought evolution.

It is worth underlining that the CMIP6 MMM depicts a larger increasing signal (>5 events decade $^{-1}$) compared to WFDE5, particularly in the southern Mediterranean at all studied time scales. These differences can be related to several factors, including models' performances, the paucity of observations in North African countries, and the reported tendency in the ESMs to underestimate precipitation-based drought persistence at monthly to decadal scales^{54,55}. Furthermore, we detected an overestimation of the warming trend by CMIP6 MMM compared to WFDE5 (Supplementary Figure 1). All these contributions can have a role in enhancing the drought representation in the ESMs (See Supplementary Table 3).

For the projection period 2021–2060, overall, the frequency of drought occurrences ranged between 55 and 125 months of 40 years, i.e., about 12–25% of the studied period (Fig. 2). The obtained result depicts considerable differences between investigated scenarios, particularly for agricultural and hydrological droughts. However, fewer differences were observed in

meteorological drought among all scenarios over the Mediterranean countries.

To better understand the projected change relative to the historic drought, we report in Fig. 3 the probability density function (PDF) for the drought frequencies over the Mediterranean domain (Land only) from the WFDE5 and CMIP6 MMM for both historical and projection periods. Further, the spatial changes in drought frequency patterns are reported in Supplementary Fig. 2.

For the meteorological drought, the CMIP6 MMM shows an evident change in variance for all considered scenarios compared to the historic period, while no significant change in the frequency was detected. On the other hand, the agricultural drought timescale and SSP scenarios show remarkable differences from each other. SSP1 and SSP2 scenarios show a pronounced change in the variance with a slight shift in drought frequency compared to the historic period. However, SSP3 and SSP5 are characterized by bimodal distribution shape, showing additional peaks shifted toward a considerable increase in drought frequency and variance (Fig. 3b). The bimodal pattern also observed for the hydrological drought timescale, with increasing

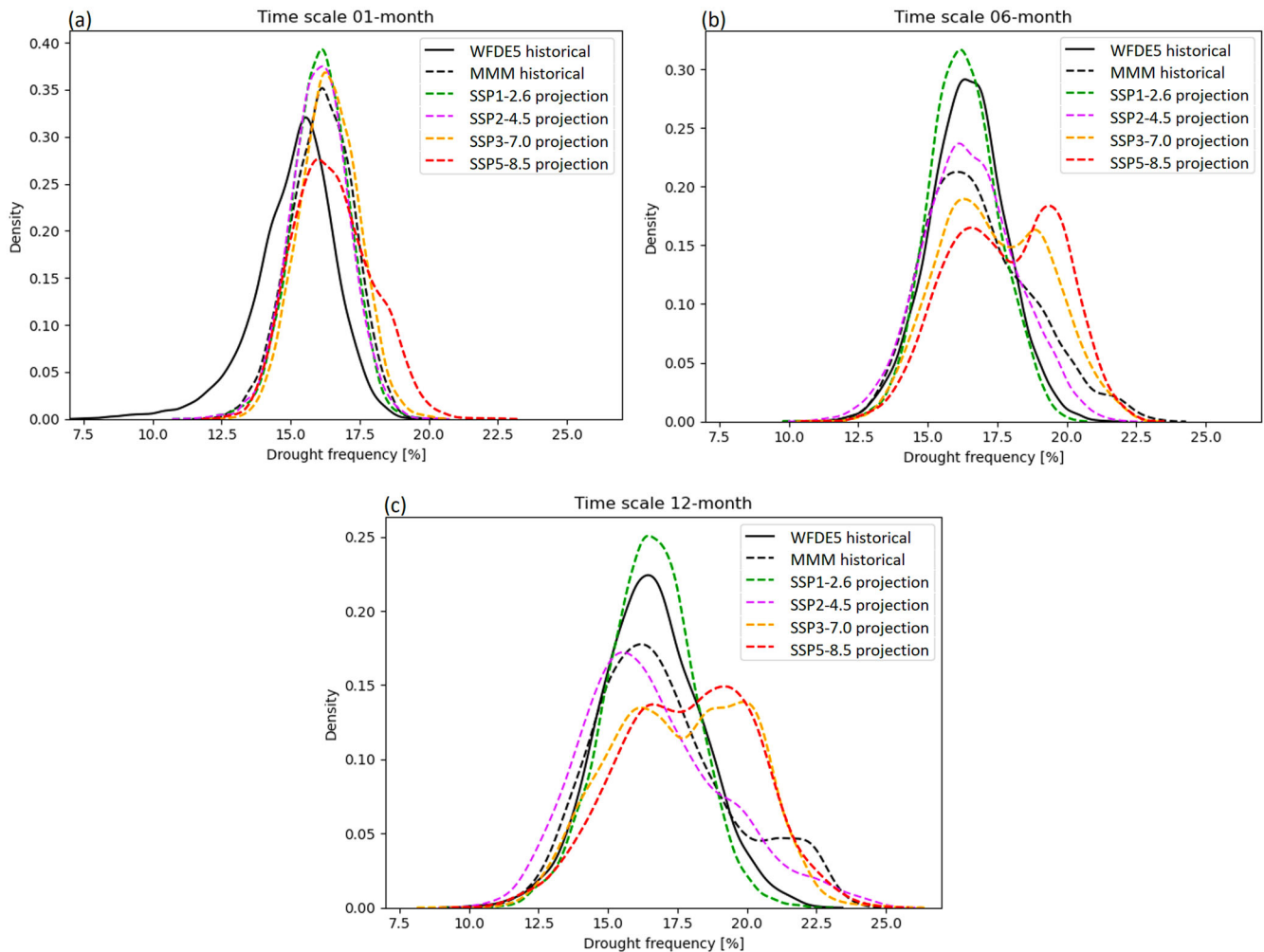


Fig. 3 Changes in drought frequency. The probability density function for drought frequency (%), using WFDE5 (solid black line) and CMIP6 MMM (dashed lines) datasets in the historical reference period 1980–2014 (black lines) and the projection period 2021–2060 under different SSP scenarios (color lines) at time scales **a** 1-month, **b** 6-months, and **c** 12-months.

variance and drought frequency maxima compared to the historical reference period. However, the low and intermediate challenging scenarios, SSP1 and SSP2, show different behaviors. SSP1 (SSP2) shows a decrease (increase) in the variance with decreasing (increasing) drought maxima. For the frequency minima, it shows a slight decrease only in SSP2 with respect to the reference period (see Fig. 3c).

The differences between the WFDE5 and CMIP6 MMM during the historical period are evident at the time scale 1-month for both drought frequency and variance pattern, and for variance only (i.e., PDF shape) at time scales 6- and 12 months. For the projection period, differences in PDFs shape are more pronounced in the aggregated timescales of SPEI; high-challenge scenarios, SSP3 and SSP5, provide comparable results, consistent with frequency maps (Fig. 2). It is challenging to provide precise reasons for changes in obtained results among scenarios. The variation in radiative forcing and socioeconomic representation among scenarios in ESMs likely the primary driver of these differences, but additional factors, such as the climate response and the non-linear approach of SPEI estimation, could have a role in the obtained patterns.

In Fig. 4, we exclude the moderate drought category from the results, focusing only on the severe and extreme dry values, i.e., $\text{SPEI} < -1.5$, to investigate the drought severity under climate change scenarios. The result shows an evident increase in the

frequency of the severe drought events with the aggregated time scales for all examined scenarios, including the low-end scenario SSP1. At the 12-month timescale, more than half of the total frequency reported in Fig. 2 is classified as severe or extreme drought over a wide area of the Mediterranean. This finding is also true at the 6-month timescale but in a less pronounced pattern. This noticeable severity over the aggregated timescales is possibly related to continuing either the heat, precipitation deficit, or both around the year; reflecting significant potential stress on the food and water systems in the near decades.

Regional SPEI time series

To deepen the analysis of the projected drought through time series reflecting the onset, duration, and intensity of drought types; we divide the domain study into four regions based on the obtained frequency and intensity results, as shown in Fig. 5, to differentiate between (1) regions that are characterized by a potential increase in drought frequency compared to the historical period (positive % in Supplementary Fig. 2), or by more than 50% of the projected drought occurrence classified as a severe or extreme drought (i.e., $\text{SPEI} < -1.5$), and (2) regions characterized by both criteria described in point 1.

We applied this criterion to the result of the worst possible scenario, SSP5–8.5 at the aggregated timescale 12-month (see

Drought intensity for the projection period 2021–2060

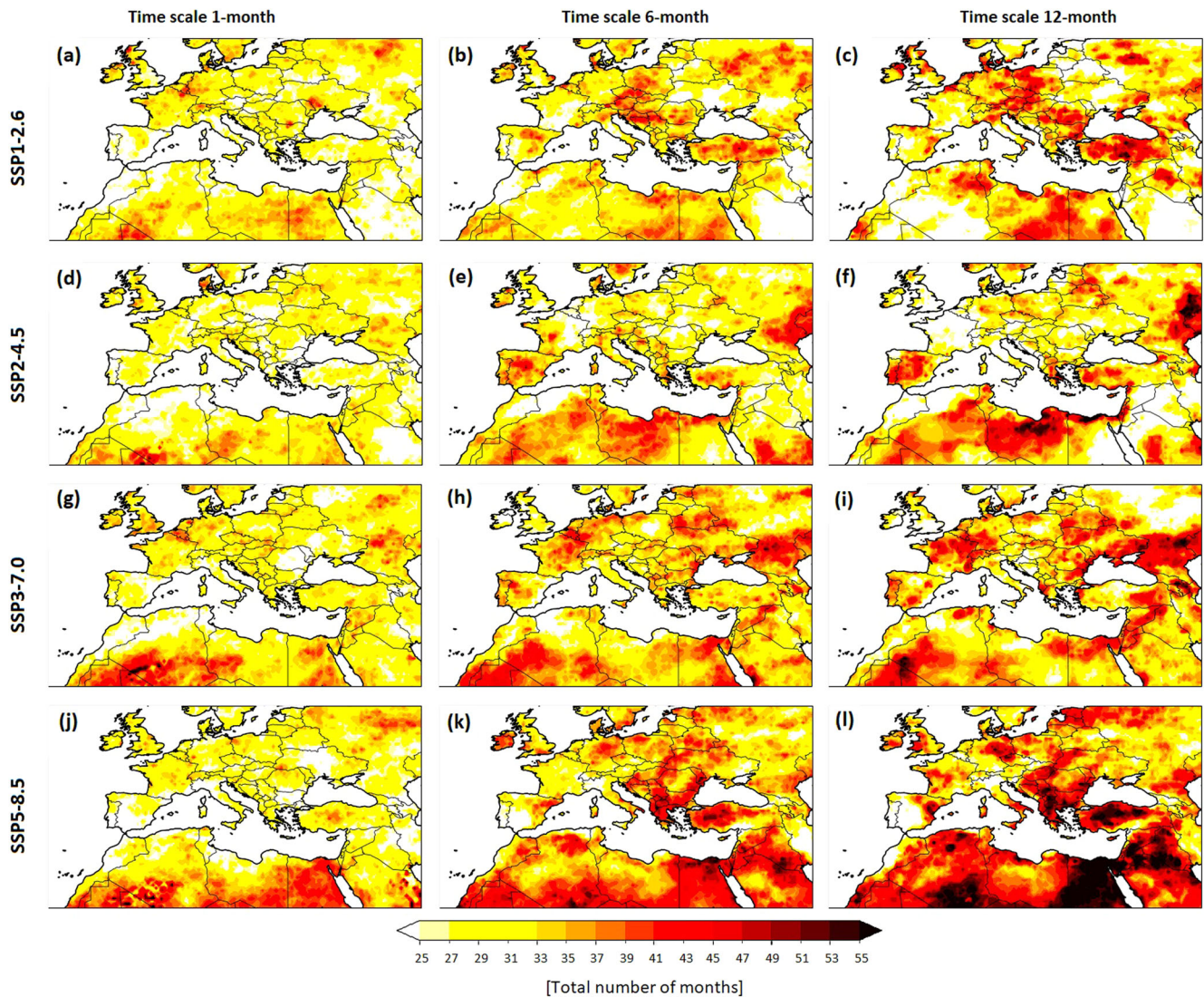


Fig. 4 Projected drought intensity. Drought frequency as a function of intensity, focusing on the severe and extreme droughts only based on the SPEI value (i.e., for $\text{SPEI} < -1.5$) at time scales 1, 6, and 12 months, spanning the projection period 2021–2060 from the CMIP6 MMM under the climate change scenarios SSP1-2.6 (a–c), SSP2-4.5 (d–f), SSP3-7.0 (g–i), and SSP5-8.5 (j–l).

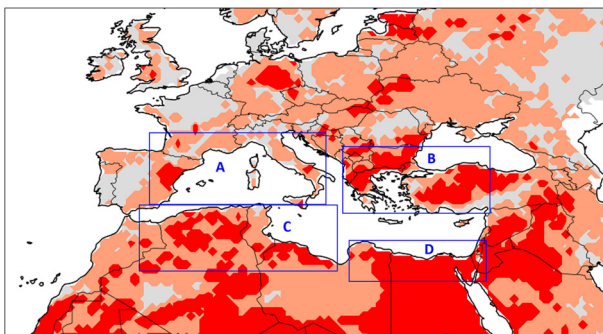


Fig. 5 Defined hotspot zones for drought in the Mediterranean. Light red areas are the regions that either show higher drought frequency in the projection period compared to the historical one or have more than 50% of projected drought events under severe classification. The dark red color indicates that both conditions are achieved in the area.

subsection ‘SPEI calculation and drought analysis,’ ‘Methods’ section).

Zone A includes parts of the countries in southwest Europe, and it is the zone that shows the least potential effect based on the defined criteria. Zones B and C are under intermediate potential impact in Europe and North Africa compared to Zone D, which lies in the eastern part of North Africa and shows the most potential adverse effects.

Figure 6 shows the monthly time series of the SPEI of the dry values only (i.e., $\text{SPEI} < -1$), thereafter SPEI-dry, during the historical period 1980–2014 using WFDE5 and CMIP6 MMM for the addressed zones. The results show a consistent pattern behavior in time scales 6 and 12 months, with higher drought frequency and stronger intensity in CMIP6 MMM compared to WFDE5. For the short time scale, the differences between the WFDE5 and CMIP6 are more pronounced, particularly in the North African zones (i.e., C and D), where a few dry events were obtained only in WFDE5 during the first half of the study period.

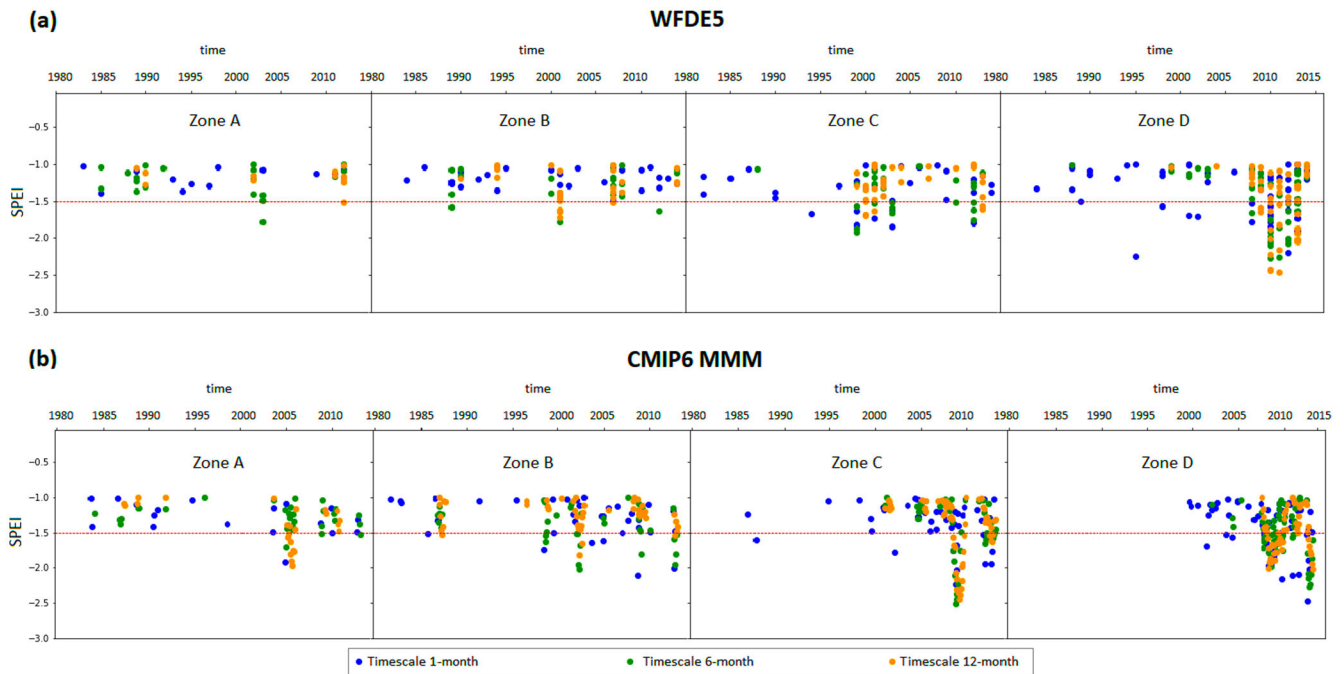


Fig. 6 Historical drought time series at a regional based. Regional SPEI-dry time series at time scales 1, 6, and 12 months, spanning the period 1980–2014, using **a** WFDE5 and **b** CMIP6 MMM datasets. The red dashed line is the upper bound of the severe values.

Nevertheless, both datasets confirm the increased tendency of dry events at all time scales and show similar behavior in the dryness profile as a function of the geographical location of the specified zones.

For the projection period, the SPEI-dry time series of Zone A shows very few drought events before 2035 at a 12-month time scale for all scenarios, while the drought occurrences are likely to be more frequent at timescales 1 and 6 months but at a mild intensity. After 2035, the drought occurrence largely increases at all timescales, and dry values tend to be more severe (Fig. 7).

In southeastern countries of the European continent (Zone B), the differences between the investigated scenarios are evident during the projected period. The SSP1–2.6 shows potential dry events in the first decade of the examined period at all timescales. After that, the time series shows improvement (i.e., decreasing drought frequency), and the drought onset is limited only at the short-scale, i.e., meteorological drought, before converting again to occurrences at longer scales by the last decade, but not as intense as the earlier one. The intermediate and high pathway scenarios, SSP3 and 5, show fewer events before 2035, which are growing with time in terms of both frequency and intensity. The extreme values concentrate on the last years of the projection period.

Zone C and D show a similar pattern to the drought profile in Zone B of the intermediate and high pathway scenarios, but with larger drought frequencies and intensity, particularly for Zone D. This is also true for the green road scenario ‘SSP1’ result of Zone C to Zone A. On the other hand, Zone D in SSP1 shows frequent drought occurrences before 2035 at all timescales, in a mild intensity, with a few exceptions. An apparent decrease followed these occurrences until 2047, before the SPEI-dry became more frequent, intense, and long-lasting onward.

Overall, the obtained results indicated that both historical and projection time series for the defined zones show a consistent behavior toward increasing the dry condition over time, but with differences in terms of variability over time, frequency, and severity among scenarios. This could be partially linked to the pronounced difference between the historical and future scenarios in PDF shapes of drought frequency shown in Fig. 3.

Further, the drought seasonality has been investigated by detecting the season(s) of the highest drought frequency during the historical and projection periods. The results indicate that dry conditions tend to occur more frequently in the boreal summer (autumn) months at the meteorological (agricultural) time scale, with a few exceptions that vary with the region and SSP scenario (Table 1). This obtained seasonality can be linked to the potential stress that would be added to summer (winter) crops in the critical phenological stages of the plants, consequently, loss in the crops’ production [e.g.,^{56,57}]. For instance, the exceptional 2022 heat and water stress of Northern Mediterranean countries that started in May and onward caused a significant loss in some strategic crops, e.g., soybean and maize^{58,59}.

Trends and correlations in climate drivers

To address the potential driver variable(s) for the drought phenomenon in the Mediterranean, we investigate the trend of the air temperature and precipitation as the climatic variables used to calculate SPEI and their correlation with the climatic water balance following^{60,61}.

A decreasing trend in the precipitation over time is evident in all considered scenarios over the European domain, particularly the Southern countries (Fig. 8). In North African countries, the precipitation trend is less pronounced, within ± 8 mm decade⁻¹, except for a few regions on the coastal area in Maghreb countries (Morocco, Algeria, and Tunisia). This small trend in absolute values may also be explained by the already low amount of precipitation this area receives under the present climate.

The temperature trend shows slight warming for the green road scenario, SSP1–2.6, within 0.3 °C decade⁻¹. Warming increases with the challenging level of future scenarios, reaching 0.8 °C decade⁻¹ for the worst possible scenario SSP5–8.5 in the Mediterranean. It is worth mentioning that the North African countries of the Mediterranean are showing comparable warming as the European domain, along with a less pronounced reduction signal in the precipitation; nonetheless, the highest deficit in the climatic water balance trend is obtained in North Africa. This is likely related to the fact that the climate in this region is mostly



Fig. 7 Projected drought time series at a regional based. Regional SPEI-dry time series at time scales 1, 6, and 12 months for zones A–D, spanning the period 2021–2060 of **a** SSP1–2.6, **b** SSP2–4.5, **c** SSP3–7.0, and **d** SSP5–8.5 scenarios. The red dashed line is the lower bound of the severe values.

arid or semi-arid; consequently, it receives a minimal amount of precipitation per year. Therefore, comparable warming can cause a more significant negative impact on the water balance. This finding is confirmed by analyzing the water balance's correlation with temperature and precipitation, which shows a stronger correlation with precipitation in the Northern Mediterranean, and with temperature in the southern Mediterranean in all SSP scenarios (Fig. 9).

DISCUSSION

The present study aims to investigate the projected characteristics of droughts over the Mediterranean in the near coming decades. To this objective, we used a multi-model mean of bias-corrected and downscaled data of five 'CMIP6' ESMs and four climate change scenarios 'SSP' for addressing the drought frequency, intensity, onset, and seasonality. The obtained results highlight an evident evolution in drought frequency and intensity, particularly for agriculture and hydrological droughts. The meteorological drought projections among the future scenarios show a remarkable change in the PDF shape of drought frequency. On the other

hand, the agriculture and hydrological droughts projections show pronounced changes in both the drought frequency mean and PDF shape, particularly for the highly challenging scenarios. These differences are driven by the response to the radiative forcing and socioeconomic challenges in future scenarios, but also, the local climate variability has a role in the obtained patterns. For instance, the driest profile for drought frequency and severity was obtained in the Southeastern Mediterranean countries, which are already about or below the water scarcity limits as addressed by the Food and Agriculture Organization of the United Nations⁶². The driver variables for the drought occurrences show a dependency on the geographical location. For instance, temperature strongly correlates with drought occurrences in the Southern Mediterranean, while precipitation correlates with drought occurrence in the Northern Mediterranean. On one side, this finding enhances the importance of considering the temperature in drought assessment, particularly in the arid or semi-arid domains where precipitation has a less important role in drought features. On the other side, it partially elucidates the evident variation between the Northern and Southern Mediterranean drought patterns. An increase in drought sensitivity could be addressed as a response

Table 1. Seasons of highest drought frequency during the historical period (Hist.) 1980–2014, and the projection period 2021–2060 for SSP scenarios.

	Meteorological drought	Agricultural drought	Hydrological drought
<i>Zone A</i>			
WFDE5 Hist.	MAM	DJF	JJA
MMM Hist.	JJA	JJA	JJA/DJF
SSP 1–2.6	JJA	JJA	DJF
SSP 2–4.5	MAM	SON	MAM
SSP3–7.7	JJA	JJA	JJA
SSP5–8.5	JJA	SON	MAM/JJA
<i>Zone B</i>			
WFDE5 Hist.	JJA	MAM	SON
MMM Hist.	JJA	JJA	JJA/DJF
SSP 1–2.6	JJA/DJF	MAM	DJF
SSP 2–4.5	JJA	DJF	MAM
SSP3–7.7	JJA	SON	DJF
SSP5–8.5	JJA	SON	SON
<i>Zone C</i>			
WFDE5 Hist.	JJA	SON	DJF/MAM
MMM Hist.	JJA	SON	DJF
SSP 1–2.6	JJA	JJA/SON	MAM
SSP 2–4.5	JJA	SON	JJA/SON
SSP3–7.7	JJA	SON	JJA
SSP5–8.5	JJA	SON	JJA/SON
<i>Zone D</i>			
WFDE5 Hist.	JJA	JJA	DJF/MAM
MMM Hist.	JJA	JJA/SON	All
SSP 1–2.6	MAM	JJA	JJA
SSP 2–4.5	JJA	SON	DJF
SSP3–7.7	JJA	SON	JJA
SSP5–8.5	JJA	SON	No seasonality

to mild or less pronounced extreme heat in the Southern Mediterranean over the next few decades as a consequence of the pointed strong relation with temperature. This conclusion aligns with the pronounced drought pattern obtained in the low challenging scenario, SSP1, for aggregated timescales.

In terms of drought seasonality, the results reveal a higher tendency in summer (autumn) months for meteorological (agricultural) droughts occurrences. This outcome reflects the logical impact of the aggregation of the dry summer conditions on the agricultural sector in autumn time, which is, for instance, consistent with the recent widespread drought over southern Europe attributed to the pronounced summer heatwave of 2022⁶³. Moreover, the compelling evidence attributed to the pace of shifting climate^{64–66} toward prolonged summertime in the Northern Hemisphere mid-latitudes⁶⁷ increases further the concern of heat stress impact on water sources and soil preservation, as well as increasing the challenge of climate adaptation.

The devastating impact due to cumulative and cascading occurrences of those drought types will not be limited only to agricultural and water sectors. In contrast, it can directly and rapidly impact energy sources that depend on water, human health⁶⁸, biodiversity, and consequently, the whole socioeconomic system of the affected countries⁶⁹, particularly the developing nations that already suffer from low adaptive and resilience capacities^{51,70}.

There is an agreement between the bias-corrected CMIP6 and reanalysis, WFDE5, for the historical period in the trend sign toward increasing the drought frequencies. However, an over-estimation in the magnitude has been obtained by CMIP6 despite the bias correction of the models, particularly in the North African countries, which is possibly linked to the greater uncertainty highlighted in Africa¹⁷.

We are aware that model data uncertainty can introduce further uncertainty in our assessment. For this reason, an ensemble of bias-corrected records has been used instead of the original single model output. Moreover, we discussed the drought frequency and severity in relative representation with the absolute values. Additional sources of the uncertainty subject to anthropogenic activities, future emission of greenhouse gases, and addressing the land-atmosphere feedback can be found [e.g., see^{71–76}].

Another potential limitation in our study concerns the AED calculation, which depended on temperature only in this work; not accounting for the impact of other variables due to limited available data, and neglecting impacts of soil moisture limitation or plant-physiological responses under higher CO₂ concentrations. This tends to result in an overestimation of magnitude and temporal trends of AED⁷⁷, with corresponding impacts on the drought assessment, in particular for stronger warming⁹.

These addressed challenges and the given complexity of quantifying drought¹⁷ to elaborate a definite description of the drought's profiles, either for the historical or projection period, should not be an argument for inaction in investigating the potential impacts and the local response for the far years. It remains beneficial and the key road for supporting countries to call for the integration of urgent adaptation and mitigation approaches to adverse climate impacts on socio-economic and vital sectors and devote efforts to reducing the uncertainties sources. Further work could aim at extending this study to include further methods of calculating the AED and drought indices, investigating the potential change in large atmospheric circulation and drought seasonality, as well as the link between climate extremes, drought occurrences, and the potential impacts.

METHODS

Data description

The WATCH Forcing Data (WFD) methodology applied to surface meteorological variables from the ERA5 reanalysis⁷⁸, WFDE5 dataset⁷⁹ is generated as a bias-corrected version of ERA5 to enhance the dataset's usability in land and hydrological applications. Except for precipitation, which is additionally bias-corrected using the Global Precipitation Climatology Center (GPCC), all the available surface variables in this dataset (e.g., temperature, cloud cover, etc.) are bias-corrected using the Climatic Research Unit (CRU) global observational dataset. The dataset of version 2 covers the period 1979–2019 with a 0.5° × 0.5° spatial resolution and hourly temporal resolution.

WFDE5 was used in this study as a reference dataset for the historical baseline period 1980–2014 to better understand the performance of the used earth system models and to enhance the reliability and interpretation of the projection results compared to the historical records.

For climate projection, we used the daily bias-adjusted temperature and precipitation data in 0.5° × 0.5° spatial resolution of the five common ESMs of CMIP6 available among the primary SSP scenarios at the time of performing the study: GFDL-ESM4, IPSL-CM6A-LR, MPI-ESM1-2-HR, MRI-ESM2-0, and UKESM1-0-LL of both historical simulation covering the period 1980–2014, and of four possible future climate and socioeconomic scenarios: SSP1–2.6, SSP2–4.5, SSP3–7.0, and SSP5–8.5 for the period 2021–2060. The bias correction and statistical downscaling applied to each CMIP6 ESMs in this study is 'ISIMIP3BASD

Decadal trends for the projection period 2021–2060

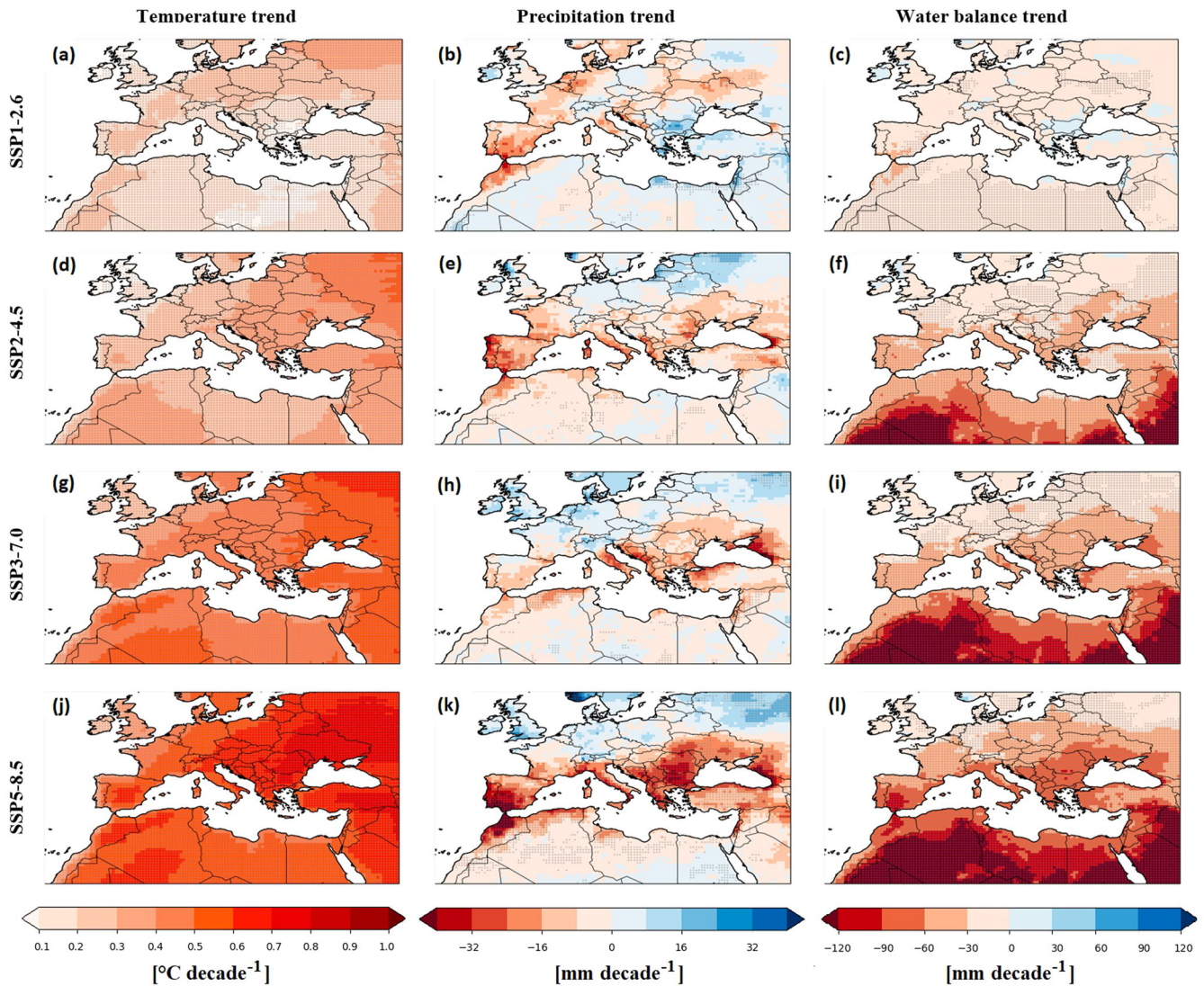


Fig. 8 Decadal trends. Temperature (left), precipitation (middle), and water balance (right) linear trends under different future scenarios: **a–c** SSP1–2.6, **d–f** SSP2–4.5, **g–i** SSP3–7.0, and **j–l** SSP5–8.5, for the projection period 2021–2060 of CMIP6 MMM. Gray dots refer to areas with a confidence interval $\geq 95\%$.

v2.5^{80,81}, which is performed by Inter-Sectoral Impact Model Intercomparison (ISIMIP). It is worth underlying that ISIMIP3BASD v2.5 also uses WFDE5 as a reference to bias-adjust CMIP6 over land⁸². The performed bias adjustment improves the homogeneity between the data records in the historical and projection simulations, consequently having a reliable assessment by climate projection [see Figs. 9–38 in ref. ⁸⁰]. Therefore, WFDE5 is preferred among other available data to be used as a reference dataset in this study.

SSP scenarios⁸³ are the latest climate change scenarios that describe the pathways of the future profile of societies⁶. SSP scenarios address the future socioeconomic challenges to adaptation and mitigation associated with Representative Concentration Pathways (RCPs) scenarios in the absence of climate or climate change policies. It is commonly represented as SSPi–j where ‘i’ indicates the socioeconomic pathway and ‘j’ indicates the radiative forcing level (in W m^{-2}).

The primary four pathways are included in this work and summarized in Table 2; the sustainability or green road scenario SSP 1, which represents low mitigation and adaptation challenges,

assuming more sustainable practices - with the low emission scenario (RCP 2.6) that assumes a cut for global CO_2 , reaching net zero after 2050. The second scenario is the middle road scenario, SSP2, which is characterized by medium adaptation and mitigation challenges - with intermediate greenhouse gases and CO_2 emissions by the end of 2050 (RCP4.5).

The high and very high emission scenarios (RCPs—7.0 and 8.5), which assume roughly double the current CO_2 by 2100 and 2050, respectively, with the rocky road scenario SSP3 of both high mitigation and adaptation challenges, and highway road SSP5 of high mitigation challenges.

The data used in this study was downloaded from the Inter-Sectoral Impact Model Intercomparison Project (ISIMIP; <https://www.isimip.org>), which was designed to assess the impacts of climate change in different sectors and at different scales⁸⁴.

SPEI calculation and drought analysis

To calculate the SPEI drought index, first, the potential evapotranspiration (PET) is estimated using the Thornthwaite method⁸⁵

Temporal correlation for the projection period 2021–2060

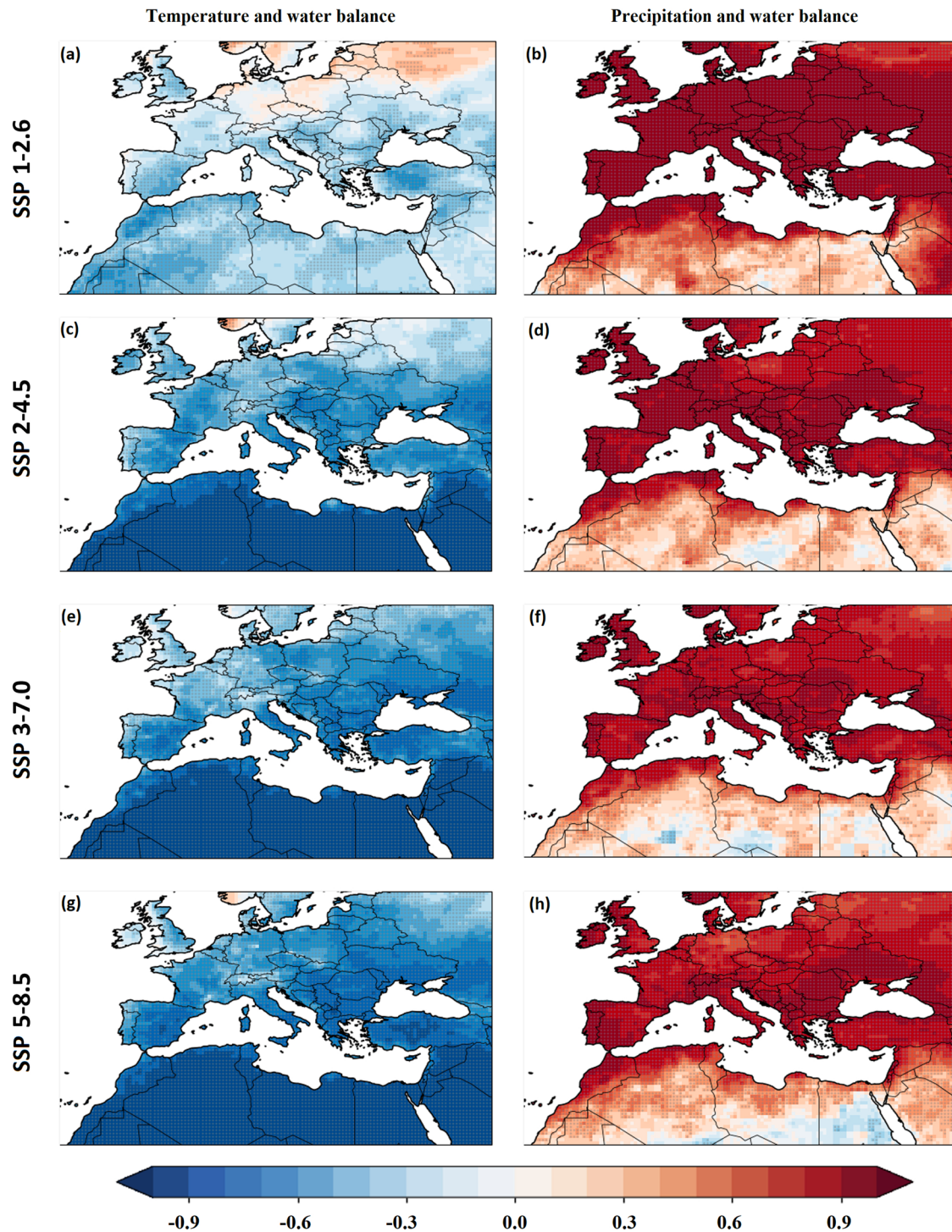


Fig. 9 Temporal correlations. Temperature (left) and precipitation (right) correlations with water balance under different future scenarios: **a, b** SSP1–2.6, **c, d** SSP2–4.5, **e, f** SSP3–7.0, and **g, h** SSP5–8.5, based on the projection period 2021–2060 of CIMP6 MMM. Gray dots refer to areas with a confidence interval $\geq 95\%$.

from both WFDE5 and CMIP6 MMM. The climatic water balance (WB) is then calculated for each month by subtracting the PET from the precipitation of each dataset and considering the scenario.

We calculate the index at three different time scales, 1, 6, and 12 months, to address the meteorological, agricultural, and hydrological droughts, respectively. The WB time series are aggregated

Table 2. Descriptive summary of the used SSP scenarios and their combinations of challenges to adaption and mitigation associated with RCP scenarios.

Scenario name	2100 climate forcing (W m ⁻²)	CO ₂ emission	Adaptation Challenge	Mitigation Challenge	Related CMIP5 RCP Scenario
SSP5-8.5	8.5	Double by 2050	Low	High	RCP 8.5
SSP3-7.0	7.0	Double by 2100	High	High	RCP 7.0
SSP2-4.5	4.5	Around current levels until 2050, then falling but not reaching net zero by 2100	Medium	Medium	RCP4.5
SSP1-2.6	2.6	Cut to net zero after 2050	Low	Low	RCP2.6

Table 3. Drought classifications based on SPEI value⁸⁶.

SPEI value	Drought classification
-1.5 < SPEI ≤ -1.0	Moderate drought
-2.0 < SPEI ≤ -1.5	Severe drought
SPEI ≤ -2.0	Extreme drought

at the required time scales (k) as follows:

$$WB_{ij}^k = \sum_{l=13-k+j}^{12} WB_{i-1,l} + \sum_{l=1}^j WB_{i,l} \quad \text{if } j < k \text{ and} \quad (1)$$

$$WB_{ij}^k = \sum_{l=j-k+1}^j WB_{i,l} \quad \text{if } j \geq k \text{ and} \quad (2)$$

where j is the month, and i is the year.

To standardize the aggregate water balance time series (WB_{ij}^k) for the specified timescales and obtain the SPEI, the probability distribution of three parameters log-logistic distributed variable (α , β , and γ) computed using the L-moment procedure following⁵⁰, and SPEI is expressed as

$$SPEI = W - \frac{C_0 + C_1 W + C_2 W^2}{1 + d_1 W + d_2 W^2 + d_3 W^3} \quad (3)$$

And $W = \sqrt{-2\ln(P)}$ for $P \leq 0.5$; where P is the probability of exceeding a determined WB value, if $P > 0.5$, then P is replaced by $1 - P$, and the sign of the resultant SPEI is reversed. The constants C_0 , C_1 , C_2 , d_1 , d_2 , and d_3 are 2.515517, 0.802853, 0.010328, 1.432788, 0.189269, and 0.001308, respectively.

The WB standardization and SPEI calculation is done for the historical and projection periods independently. The drought severity has been classified according to the SPEI value⁸⁶, as shown in Table 3.

For each timescale, the drought frequency and intensity were evaluated. The drought frequency was calculated by counting the number of times that SPEI values below -1 in each grid cell during the studied historical and projection periods, 1980–2014 and 2021–2060.

The drought intensity is defined based on the SPEI values, as shown in Table 3. The relative values for both drought frequency and intensity are discussed as the number of detected events per period divided by the total number of months of a whole period.

Analyzing the time series for the SPEI has been done on a regional basis; addressing the drought onset, duration, and severity. Dividing the study area into sub-regions is crucial, whereas average different drought severity levels can mislead the interpretation of the results. The sub-region selection is based on the drought frequency and intensity, as explained in Fig. 5, to differentiate between regions characterized by frequent and intense drought and regions of frequent mild drought. The average for the SPEI values is calculated corresponding to the defined zones in Fig. 5 (coordinates of each zone are shown in Supplementary Table 1). To do so, we select the grid cells that

show the total number of months with SPEI-value < -1.5 , more than 50% of the total number of dry SPEI values, i.e., when severe or extreme drought frequency is higher than moderate drought frequency, and simultaneously show a relative frequency in the projection period higher than the historical period, to be labeled as the first-order of vulnerable spots. The grids that show only one availability of the defined conditions are labeled as second-order vulnerable spots. The hotspot zones are defined on the basis of having maximum consistent order of vulnerability in each zone to reduce as possible the effect of SPEI averaging over the domain, taking into account the geographical location.

Finally, we investigate the linear trends and correlation of the climate variables used in calculating SPEI (i.e., temperature, precipitation, and water balance), with Mann–Kendall and P -value statistical test for their significance, to understand the driving variable for the drought phenomenon in Mediterranean countries.

DATA AVAILABILITY

All bias-adjusted atmospheric climate input data of ISIMIP (version 1.1) for both historical and future climate simulations are available on ISIMIP Repository: https://data.isimip.org/search/time_step/daily/product/InputData/. DOI: <https://doi.org/10.48364/ISIMIP.842396.1>. WFDE5 Version 2.0 is available at Copernicus Climate Change Service (C3S) Climate Data Store (CDS): <https://cds.climate.copernicus.eu/cdsapp#!/dataset/derived-near-surface-meteorological-variables?tab=form>, DOI: <https://doi.org/10.24381/cds.20d54e34>. The post-processed and analyzed data that support the findings of this study are available from the corresponding author upon reasonable request.

CODE AVAILABILITY

The computation of the PET and of SPEI has been done with the Climate Indices python package (https://github.com/monocongo/climate_indices; version 1.0.10). Moreover, the postprocessing of the ESM data and SPEI results have been done with the Climate Data Operators (CDO: <https://code.mpimet.mpg.de/projects/cdo>) and the corresponding Python scripts for visualizing the results. The used tools and packages are freely available.

Received: 4 May 2023; Accepted: 15 August 2023;

Published online: 07 September 2023

REFERENCES

- Cavus, Y. & Aksoy, H. Critical drought severity/intensity-duration-frequency curves based on precipitation deficit. *J. Hydrol.* **584**, 124312 (2020).
- Cavus, Y., Stahl, K. & Aksoy, H. Drought intensity-duration-frequency curves based on deficit in precipitation and streamflow for water resources management. *Hydrol. Earth Syst. Sci. Discuss.* (in review) (2023).
- Gevaert, A. I., Veldkamp, T. I. E. & Ward, P. J. The effect of climate type on timescales of drought propagation in an ensemble of global hydrological models. *Hydrol. Earth Syst. Sci.* **22**, 4649–4665 (2018).
- Wang, Q. et al. An improved daily standardized precipitation index dataset for mainland China from 1961 to 2018. *Sci. Data* **9**, 124 (2022).
- Vicente-Serrano, S. M., Quiring, S., Peña-Gallardo, M., Yuan, S. & Dominguez-Castro, F. A review of environmental droughts: Increased risk under global warming? *Earth Sci. Rev.* **201**, 102953 (2020a).

6. IPCC. The Physical science basis, Climate Change 2021. Contribution of working group I to the sixth assessment report of the intergovernmental panel on climate change (2021).
7. Cos, J. et al. The Mediterranean climate change hotspot in the CMIP5 and CMIP6 projections. *Earth Syst. Dynam.* **13**, 321–340 (2022).
8. Lionello, P. & Scarascia, L. The relation between climate change in the Mediterranean region and global warming. *Reg. Environ. Change* **18**, 1481–1493 (2018).
9. Seneviratne, S. I. et al. Weather and Climate Extreme Events in a Changing Climate, Climate Change 2021: The Physical Science Basis. Contribution of Working Group I to the Sixth Assessment Report of the Intergovernmental Panel on Climate Change (eds Masson-Delmotte, V. et al.) (2021).
10. Toreti, A. et al. Drought in Europe August 2022: GDO analytical report. (Publications Office of the European Union, Joint Research Centre, Luxembourg, 2022).
11. Giorgi, F. & Lionello, P. Climate change projections for the Mediterranean region. *Glob. Planet. Change* **63**, 90–104 (2008).
12. Boé, J. & Terray, L. Land-sea contrast, soil-atmosphere and cloud-temperature interactions: Interplays and roles in future summer European climate change. *Clim. Dynam.* **42**, 683–699 (2014).
13. Ali, E. et al. Cross-Chapter Paper 4: Mediterranean Region, Climate Change 2022: Impacts, Adaptation and Vulnerability. Contribution of Working Group II to the Sixth Assessment Report of the Intergovernmental Panel on Climate Change (eds Pörtner, H.-O. et al.). Cambridge University Press, Cambridge, UK and New York, NY, USA, 2233–2272 (2022).
14. Barros, V. et al. Impacts, Adaptation, and Vulnerability, Climate Change 2014. Part B: Regional Aspects. Contribution of Working Group II to the Fifth Assessment Report of the Intergovernmental Panel on Climate Change (eds Barros, V. R. et al.) (2014).
15. Trambly, Y. et al. Challenges for drought assessment in the Mediterranean region under future climate scenarios. *Earth Sci. Rev.* **210**, 103348 (2020).
16. Stahl, K. et al. The challenges of hydrological drought definition, quantification and communication: an interdisciplinary perspective. *Proc. Int. Assoc. Hydrol.* **383**, 291–295 (2020).
17. Vicente-Serrano, S. M. et al. Global drought trends and future projections. *Philos. Trans. R. Soc. A* **380**, 20210285 (2022).
18. Vicente-Serrano, S. M., Van der Schrier, G., Beguería, S., Azorin-Molina, C. & Lopez-Moreno, J.-I. Contribution of precipitation and reference evapotranspiration to drought indices under different climates. *J. Hydrol.* **526**, 42–54 (2014).
19. Li, L., She, D., Zheng, H., Lin, P. & Yang, Z. Elucidating diverse drought characteristics from two meteorological drought indices (SPI and SPEI) in China. *J. Hydrol.* **21**, 1513–1530 (2020).
20. Ahmadalipour, A., Moradkhani, H. & Demirel, M. C. A comparative assessment of projected meteorological and hydrological droughts: elucidating the role of temperature. *J. Hydrol.* **553**, 785–797 (2017).
21. Ahmadalipour, A., Moradkhani, H. & Svoboda, M. Centennial drought outlook over the CONUS using NASA-NEX downscaled climate ensemble. *Int. J. Climatol.* **37**, 2477–2491 (2016).
22. Diffenbaugh, N. S., Swain, D. L. & Touma, D. Anthropogenic warming has increased drought risk in California. *Proc. Natl Acad. Sci. USA* **112**, 201422385 (2015).
23. Dai, A. Drought under global warming: a review. *WIREs Rev. Clim. Chang.* **2**, 45–65 (2011).
24. Faiz, M. et al. A composite drought index developed for detecting large-scale drought characteristics. *J. Hydrol.* **605**, 127308 (2022).
25. Ahmad, F. M., Shen, R., Zaheer, A. B., Ahmad, N. M. & Zhang, Y. Study capability of Standardized Precipitation Evapotranspiration Index to represent soil moisture variability during winter season over Pakistan for the period 1951–2010. *Meteorol. Atmos. Phys.* **130**, 689–699 (2018).
26. Ariyanto, D. P., Aziz, A., Komariah, K., Sumani, S. & Abara, M. Comparing the accuracy of estimating soil moisture using the Standardized Precipitation Index (SPI) and the Standardized Precipitation Evapotranspiration Index (SPEI). *SAINS TANAH- Stjssa.* **17**, 23–29 (2020).
27. Gao, Y. et al. Assessing various drought indicators in representing summer drought in boreal forests in Finland. *Hydrol. Earth Syst. Sci.* **20**, 175–191 (2016).
28. Xu, Z.-G., Wu, Z.-Y., He, H., Gu, X. & Zhang, Y.-L. Comparison of soil moisture at different depths for drought monitoring based on improved soil moisture anomaly percentage index. *Water Sci. Eng.* **14**, 171–183 (2021).
29. Polade, S. D., Gershunov, A., Cayan, D. R., Dettinger, M. D. & Pierce, D. W. Precipitation in a warming world: assessing projected hydro-climate changes in California and other Mediterranean climate regions. *Sci. Rep.* **7**, 10783 (2017).
30. James, R. & Washington, R. Changes in African temperature and precipitation associated with degrees of global warming. *Clim. Change* **117**, 859–872 (2013).
31. Maúre, G. et al. The southern African climate under 1.5°C and 2°C of global warming as simulated by CORDEX regional climate models. *Environ. Res. Lett.* **13**, 065002 (2018).
32. Kirtman, B. et al. Near-term Climate Change: Projections and Predictability, Climate Change 2013: The Physical Science Basis. Contribution of Working Group I to the Fifth Assessment Report of the Intergovernmental Panel on Climate Change (eds Stocker, T. F., et al.) (2013).
33. Collins, M. et al. Long-term Climate Change: Projections, Commitments and Irreversibility, Climate Change 2013: The Physical Science Basis. Contribution of Working Group I to the Fifth Assessment Report of the Intergovernmental Panel on Climate Change (eds Stocker, T. F., et al.) (2013).
34. Knutson, T. & Zeng, F. Model assessment of observed precipitation trends over land regions: detectable human influences and possible low bias in model trends. *J. Clim.* **31**(12), 4617–4637 (2018).
35. Orlovsky, B. & Seneviratne, S. Elusive drought: Uncertainty in observed trends and short- and long-term CMIP5 projections. *Hydrol. Earth Syst. Sci.* **17**, 1765–1781 (2013).
36. Eyring, V. et al. Overview of the coupled model intercomparison project phase 6 (CMIP6) experimental design and organization. *Geosci. Model Dev.* **9**, 1937–1958 (2016).
37. Li, H. et al. Drylands face potential threat of robust drought in the CMIP6 SSPs scenarios. *Environ. Res. Lett.* **16**, 114004 (2021).
38. Müller, C. et al. Exploring uncertainties in global crop yield projections in a large ensemble of crop models and CMIP5 and CMIP6 climate scenarios. *Environ. Res. Lett.* **16**, 3 (2021).
39. Hou, M. & Tang, Y. Recent progress in simulating two types of ENSO—from CMIP5 to CMIP6. *Front. Mar. Sci.* **9**, 986780 (2022).
40. Li, J., Huo, R., Chen, H., Zhao, Y. & Zhao, T. Comparative assessment and future prediction using CMIP6 and CMIP5 for annual precipitation and extreme precipitation simulation. *Front. Earth Sci.* **9**, 687976 (2021).
41. Fan, X., Miao, C., Duan, Q., Shen, C. & Wu, Y. The performance of CMIP6 versus CMIP5 in simulating temperature extremes over the global land surface. *J. Geophys. Res. Atmos.* **125**, 33031 (2020).
42. Jiang, D., Hu, D., Tian, Z. & Lang, X. Differences between CMIP6 and CMIP5 models in simulating climate over China and the East Asian monsoon. *Adv. Atmos. Sci.* **37**, 1102–1118 (2020).
43. Xin, X., Wu, T., Zhang, J., Yao, J. & Fang, Y. Comparison of CMIP6 and CMIP5 simulations of precipitation in China and the East Asian Summer Monsoon. *Int. J. Climatol.* **40**, 6423–6440 (2020).
44. Moss, R. H. et al. The next generation of scenarios for climate change research and assessment. *Nature* **463**, 747 (2010).
45. Riahi, K. et al. The shared socioeconomic pathways and their energy, land use, and greenhouse gas emissions implications: an overview. *Glob. Environ. Change* **42**, 153–168 (2017).
46. Van Vuuren, D. P. et al. Winkler A new scenario framework for climate change research: scenario matrix architecture. *Clim. Change* **122**, 373–386 (2014).
47. Cook, B. I. et al. Twenty-first century drought projections in the CMIP6 forcing scenarios. *Earth's Fut.* **8**, e2019EF001461 (2020).
48. Wang, T., Tu, X., Singh, V. P., Chen, X. & Lin, K. Global data assessment and analysis of drought characteristics based on CMIP6. *J. Hydrol.* **596**, 126091 (2021).
49. Ukkola, A. M., De Kauwe, M. G., Roderick, M. L., Abramowitz, G. & Pitman, A. J. Robust future changes in meteorological drought in CMIP6 projections despite uncertainty in precipitation. *Geophys. Res. Lett.* **47**, e2020GL087820 (2020).
50. Vicente-Serrano, S. M., Beguería, S. & López-Moreno, J.-I. A multi-scalar drought index sensitive to global warming: the standardized precipitation evapotranspiration index - SPEI. *J. Clim.* **23**, 1696–1718 (2010).
51. Perkins-Kirkpatrick, S. E. & Lewis, S. C. Increasing trends in regional heatwaves. *Nat. Commun.* **11**, 3357 (2020).
52. Sanches, F. H. C., Martins, F. R., Conti, W. R. P. & Christofolletti, R. A. The increase in intensity and frequency of surface air temperature extremes throughout the western South Atlantic coast. *Sci. Rep.* **13**, 6293 (2023).
53. Tamm, O., Saaremaa, E., Rahkema, K., Jaagus, J. & Tamm, T. The intensification of short-duration rainfall extremes due to climate change – Need for a frequent update of intensity–duration–frequency curves. *Clim. Serv.* **30**, 100349 (2023).
54. Moon, H., Gudmundsson, L. & Seneviratne, S. Drought persistence errors in global climate models. *J. Geophys. Res. Atmos.* **123**, 3483–3496 (2018).
55. Ault, T. R., Cole, J., Overpeck, J., Pederson, G. & Meko, D. Assessing the risk of persistent drought using climate model simulations and paleoclimate data. *J. Clim.* **27**, 7529–7549 (2014).
56. Santini, M., Noce, S., Antonelli, M. & Caporaso, L. Complex drought patterns robustly explain global yield loss for major crops. *Sci. Rep.* **12**, 5792 (2022).
57. Schumacher, D., Zachariah, M. & Otto, F. High temperatures exacerbated by climate change made 2022 Northern Hemisphere droughts more likely. (World Weather Attribution, United Kingdom, 2022).

58. Faranda, D., Pascale, S. & Bulut, B. Persistent anticyclonic conditions and climate change exacerbated the exceptional 2022 European-Mediterranean drought. *Environ. Res. Lett.* **18**, 034030 (2023).
59. Bettina, B. et al. JRC MARS Bulletin—Crop monitoring in Europe—July 2022. *Publ. Off. Eur. Union Jt. Res. CentLuxemb.* **30**, 7 (2022).
60. Tan, C., Yang, J. & Li, M. Temporal-spatial variation of drought indicated by SPI and SPEI in Ningxia Hui autonomous region, China. *Atmosphere* **6**, 1399–1421 (2015).
61. Liu, X., Xu, Z. & Yu, R. Spatiotemporal variability of drought and the potential climatological driving factors in the Liao River basin. *Hydrol. Process.* **26**, 1–14 (2012).
62. FAO. Towards a Regional Collaborative Strategy on Sustainable Agricultural Water Management and Food Security in the Near East and North Africa Region. Second edition (2015).
63. Schumacher, D. et al. Detecting the human fingerprint in the summer 2022 West-Central European soil drought. *EGUsphere*, preprint at <https://doi.org/10.5194/egusphere-2023-717> (2023).
64. Stine, A., Huybers, P. & Fung, I. Changes in the phase of the annual cycle of surface temperature. *Nature* **457**, 435–440 (2009).
65. Burrows, M. T. et al. The pace of shifting climate in marine and terrestrial ecosystems. *Science* **334**, 652–655 (2011).
66. Woolway, R. I. The pace of shifting seasons in lakes. *Nat. Commun.* **14**, 2101 (2023).
67. Wang, J. et al. Changing lengths of the four seasons by global warming. *Geophys. Res. Lett.* **48**, e2020GL091753 (2021).
68. McMichael, A. J. & Lindgren, E. Climate change: present and future risks to health, and necessary responses. *J. Intern. Med.* **270**, 401–413 (2011).
69. Madruga de Brito, M. Compound and cascading drought impacts do not happen by chance: A proposal to quantify their relationships. *Sci. Total Environ.* **778**, 146236 (2021).
70. IPCC. Impacts, Adaptation and Vulnerability, Climate Change 2022. Contribution of Working Group II to the Sixth Assessment Report of the Intergovernmental Panel on Climate Change (2022).
71. Gimeno-Sotelo, L. et al. Assessment of the global coherence of different types of droughts in model simulations under a high anthropogenic emission scenario. *Authorea*, preprint at <https://doi.org/10.22541/essoar.167810352.25033492/v1> (2023).
72. AghaKouchak, A. et al. Anthropogenic drought: Definition, challenges, and opportunities. *Rev. Geophys.* **59**, e2019RG000683 (2021).
73. Zhou, S. et al. Soil moisture–atmosphere feedbacks mitigate declining water availability in drylands. *Nat. Clim. Chang.* **11**, 38–44 (2021).
74. Vicente-Serrano, S. M. et al. Global characterization of hydrological and meteorological droughts under future climate change: The importance of time-scales, vegetation–CO₂ feedbacks and changes to distribution functions. *Int. J. Climatol.* **40**(5), 2557–2567 (2020b).
75. Margariti, J., Rangecroft, S., Parry, S., Wendt, D. E. & Van Loon, A. F. Anthropogenic activities alter drought termination. *Elem. Sci. Anth* **27**, 7–27 (2019).
76. Berg, A. et al. Land–atmosphere feedbacks amplify aridity increase over land under global warming. *Nat. Clim. Chang.* **6**, 869–874 (2016).
77. Sheffield, J., Wood, E. & Roderick, M. Little change in global drought over the past 60 years. *Nature* **491**, 435–438 (2012).
78. Hersbach, H. et al. The ERA5 global reanalysis. *Q. J. R. Meteorol.* **146**, 1999–2049 (2020).
79. Cucchi, M. et al. WFDE5: bias-adjusted ERA5 reanalysis data for impact studies. *Earth Syst. Sci. Data.* **12**, 2097–2120 (2020).
80. Lange, S. ISIMIP3b bias adjustment fact sheet. (2021).
81. Lange, S. Trend-preserving bias adjustment and statistical downscaling with ISIMIP3BASD (v1.0). *Geosci. Model Dev.* **12**, 3055–3070 (2019).
82. Lange, S. et al. WFDE5 over land merged with ERA5 over the ocean (W5E5 v2.0). *ISIMIP Repository* (2020).
83. O'Neill, B. C. et al. The Scenario Model Intercomparison Project (ScenarioMIP) for CMIP6. *GMD* **9**, 3461–3482 (2016).
84. Warszawski, L. et al. The Inter-Sectoral Impact Model Intercomparison Project (ISI-MIP): project framework. *Proc. Natl Acad. Sci. USA* **11**, 3228–3232 (2013).
85. Thornthwaite, C. W. An approach toward a rational classification of climate. *Geogr. Rev.* **38**, 55–94 (1948).
86. Essa, Y. H., Khalil, A. & Abdel-Wahab, M. Assessment of agricultural drought under climate change. *Res. J. Fish. Hydrobiol.* **11**, 1–11 (2016).

ACKNOWLEDGEMENTS

We acknowledge the Working Group on Coupled Modeling of the World Climate Research Program, which is responsible for the CMIP products. Additionally, we gratefully acknowledge the ISIMIP Project and community (ISIMIP; www.isimip.org) for their roles in producing bias-adjusted and downscale model data and making them available, from which input data were used to perform the study. We also thank Smart Agriculture based on Meteorological Big Data (ID_43088) supported by STDF, the EQC contract C3S_511_CNR, and C3S2_520_CNR Copernicus Climate Services for their financial support and for sparking the idea that led to this study.

AUTHOR CONTRIBUTIONS

Y.H.E.: Conceptualization, data curation, formal analysis, interpreted the results, investigation, methodology, and writing—original draft; M.H.: Conceptualization, methodology, interpreted the results, and writing—review and editing; W.T.: Conceptualization, methodology, interpreted the results, and writing—review and editing; A.M.E.: Conceptualization, investigation, interpreted the results, and writing—review and editing; and C.Y.: Conceptualization, resources, interpreted the results, and writing—review and editing.

COMPETING INTERESTS

The authors declare no competing interests.

ADDITIONAL INFORMATION

Supplementary information The online version contains supplementary material available at <https://doi.org/10.1038/s41612-023-00458-4>.

Correspondence and requests for materials should be addressed to Yassmin H. Essa.

Reprints and permission information is available at <http://www.nature.com/reprints>

Publisher's note Springer Nature remains neutral with regard to jurisdictional claims in published maps and institutional affiliations.



Open Access This article is licensed under a Creative Commons Attribution 4.0 International License, which permits use, sharing, adaptation, distribution and reproduction in any medium or format, as long as you give appropriate credit to the original author(s) and the source, provide a link to the Creative Commons license, and indicate if changes were made. The images or other third party material in this article are included in the article's Creative Commons license, unless indicated otherwise in a credit line to the material. If material is not included in the article's Creative Commons license and your intended use is not permitted by statutory regulation or exceeds the permitted use, you will need to obtain permission directly from the copyright holder. To view a copy of this license, visit <http://creativecommons.org/licenses/by/4.0/>.

© The Author(s) 2023